Published in : Molecular Human Reproduction (2026), vol. 32, issue 1, gaag009
doi.org/10.1093/molehr/gaag009
Status : Postprint (Author's version)

STAGE-DEPENDENT SPHINGOSINE-1-PHOSPHATE PATHWAY MODULATION AS A THERAPEUTIC STRATEGY IN A MURINE MODEL OF ADENOMYOSIS

Marlyne Squatrito[1], Silvia Blacher[1], Julie Vervier[1,2], Laetitia Bernet[1], Alessandra Camboni[3,4], Marie-Madeleine Dolmans[3,5], and Carine Munaut[1,*]

[1]*Laboratory of Biology of Tumor and Development, GIGA-Cancer, University of Liège, Liège, Belgium*
[2]*Department of Obstetrics and Gynecology, Hôpital de la Citadelle, University of Liège, Liège, Belgium*
[3]*Gynecology Research Unit, Institut de Recherche Experimentale et Clinique, Université Catholique de Louvain, Brussels, Belgium*
[4]*Anatomopathology Department, Cliniques Universitaires Saint-Luc, Brussels, Belgium*
[5]*Gynecology Department, Cliniques Universitaires Saint-Luc, Brussels, Belgium*
**Correspondence address. Laboratory of Biology of Tumor and Development, GIGA-Cancer, University of Liege, Avenue Hippocrate 13, 4000 Liège, Belgium. E-mail: c.munaut@uliege.be - https://orcid.org/0000-0003-4952-9637*

Abstract

Adenomyosis is characterized by chronic inflammation, myometrial remodeling, and subfertility, yet therapeutic options that preserve reproductive potential remain limited. Sphingosine-1-phosphate (S1P) signaling regulates immune-cell trafficking, vascular remodeling, and tissue invasion, but its contribution to adenomyosis remains poorly defined. This study investigated the temporal regulation of this pathway in a tamoxifen-induced murine model of adenomyosis and evaluated whether its pharmacological inhibition alters uterine immune profiles and lesion severity. A total of 122 female CD1 mice were used (79 adenomyosis, 43 control). Preventive treatment (with FTY720) started at weaning, while therapeutic interventions (with FTY720 and SKI-5C) were initiated at 6weeks. Outcomes included body/uterine weight, lesion prevalence, grading and depth, immune-cell phenotyping by flow cytometry, and uterine expression of inflammatory, angiogenic, and invasion-associated genes. Early disease (at 4weeks) was marked by increased expression of S1PR1/2 and downregulation of SGPL, while established disease (at 12weeks) showed that S1PR1 remained elevated with additional upregulation of SPHK1 and S1PR4. Preventive FTY720 reduced lesion depth and grade, whereas therapeutic SKI-5C decreased lesion prevalence and invasion. Uterine weight remained reduced across adenomyosis groups and was not restored by treatment. Immune profiling revealed no major differences in total T-cell abundance between the control and adenomyosis groups. However, SKI-5C treatment was associated with the most pronounced modulation of uterine immune cells, particularly affecting T- and NK-cell-related subsets. Gene expression analyses demonstrated increased interleukin-6 in early disease and modulation of urokinase-type plasminogen activator associated with the treatments. Study limitations included constraints related to immune-cell recovery from uterine tissue, the relatively short duration of treatment, and translational differences between murine and human adenomyosis. Overall, these findings indicate that S1P signaling contributes to immune microenvironment remodeling and lesion progression in adenomyosis. These results support S1P pathway modulation as a promising therapeutic strategy meriting evaluation in human studies.

Keywords:

Adenomyosis, murine model, sphingosine-1-phosphate signaling, FTY720, SKI-5C, uterine immune profiling, myometrium remodeling

Published in : Molecular Human Reproduction (2026), vol. 32, issue 1, gaag009
doi.org/10.1093/molehr/gaag009
Status : Postprint (Author's version)

Graphical abstract

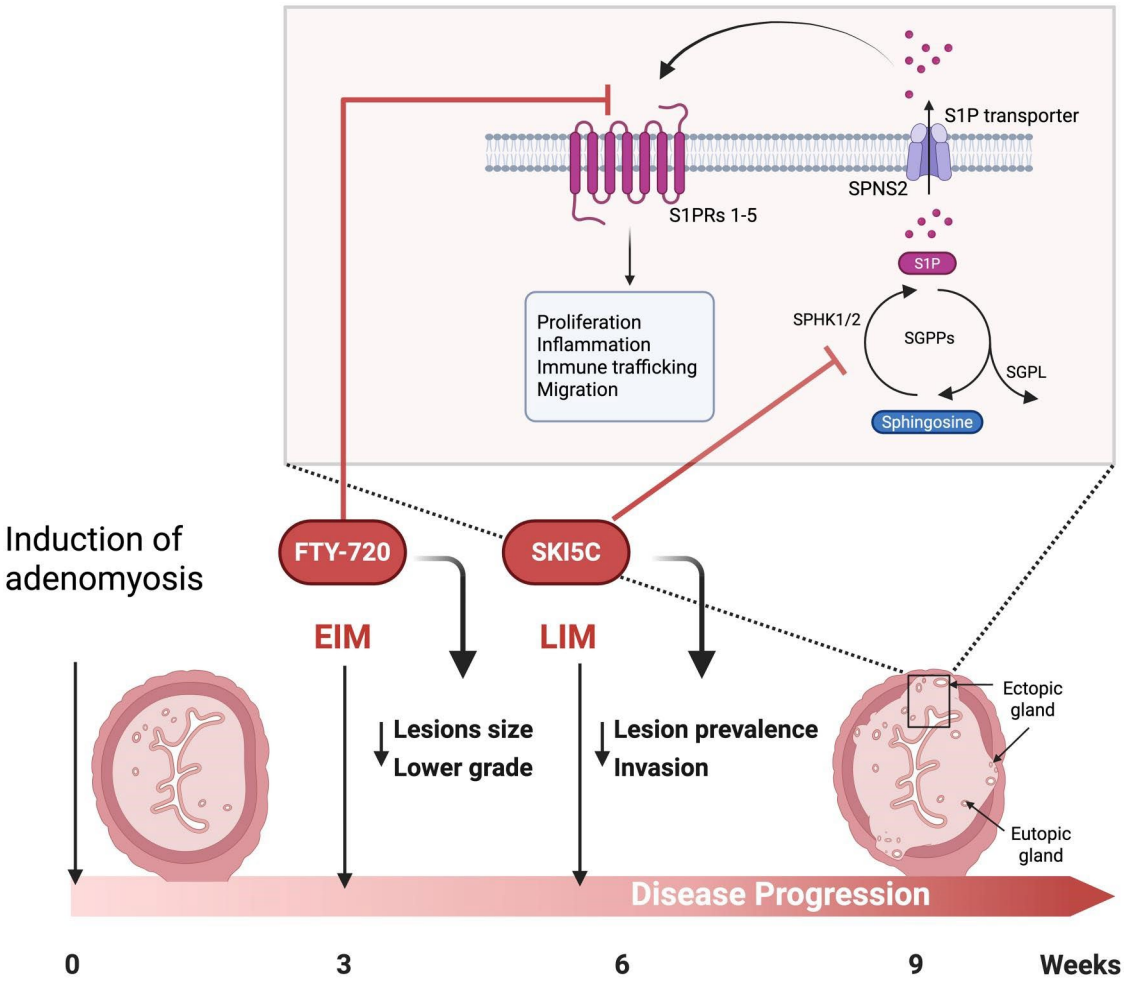

Stage-dependent modulation of sphingosine-1-phosphate (S1P) signaling in a murine adenomyosis model reveals distinct preventive and therapeutic effects of FTY720 and SKI-5C on lesion progression and uterine immune remodeling. S1P, sphingosine-1-phosphate; S1PR, sphingosine- 1-phosphate receptor; SPHK, sphingosine kinase; SGPL, sphingosine-1-phosphate lyase; EIM, early intervention model; LIM, late intervention model.
Created in BioRender. Munaut, C. (2026) https://BioRender.com/w3cc3a6.

Introduction

Adenomyosis is a chronic gynecological disorder characterized by the ectopic presence of endometrial glands and stroma within the myometrium (Bird *et al.*, 1972). This condition is frequently associated with dysmenorrhea, heavy menstrual bleeding, and infertility, with a substantial impact on women's quality of life (Vannuccini *et al.*, 2017). Epidemiological studies estimate a prevalence of up to 20% among women of reproductive age, though the true rates may be underestimated due to diagnostic challenges and overlap with other gynecological disorders such as endometriosis (Abbott, 2017; Loring *et al.*, 2021). Adenomyosis severity is often classified histologically based on the depth of myometrial invasion: grade 1 involves the inner third of the myometrium, grade 2 extends to the mid-myometrium, and grade 3 corresponds to deep or full-thickness invasion, with more extensive lesions typically associated with more severe symptoms (Bird *et al.*, 1972; Moawad *et al.*, 2023). Despite its frequency, current treatments are limited to hormonal therapies or hysterectomy (Vannuccini *et al.*, 2018; Sharara *et al.*, 2021), which may not be suitable for

women wishing to preserve fertility, highlighting the urgent need for alternative therapeutic strategies (Vannuccini and Petraglia, 2019).

Emerging evidence implicates chronic local inflammation, immune dysregulation, and abnormal tissue remodeling as central mechanisms driving adenomyosis progression (Zhai *et al.*, 2020). In our previous study using a tamoxifen-induced mouse model of adenomyosis, we reported alterations in uterine immune cell populations, notably in T lymphocytes and macrophages, pointing to local immune imbalance as a driver of disease progression (Squatrito *et al.*, 2025). Furthermore, transcriptomic and proteomic studies have identified dysregulation of inflammatory mediators, extracellular matrix components, and immune-related genes in adenomyotic tissues (Xiaoyu *et al.*, 2013; Bourdon *et al.*, 2021b; Liu *et al.*, 2021; Lin *et al.*, 2022). These findings suggest that crosstalk between immune responses and tissue remodeling sustains disease progression.

Among the signaling pathways potentially involved in these processes, the sphingosine-1-phosphate (S1P) axis is of particular interest (Di Paolo *et al.*, 2022). S1P is a bioactive lipid mediator that regulates immune cell trafficking, angiogenesis, vascular integrity, fibrosis, and cell migration (Spiegel and Milstien, 2011; Donati *et al.*, 2021; Gomez-Larrauri *et al.*, 2025). It is synthesized intracellularly by sphingosine kinases (SPHK1 and SPHK2) and signals through five G protein-coupled receptors (S1PR1–5), whose expression is cell type- and context-dependent (Maceyka *et al.*, 2012). While the specific roles of S1P receptors and enzymes in the human uterus remain incompletely characterized, alterations in this pathway have been reported in uterine tissues of women with adenomyosis (Vannuzzi *et al.*, 2022). Aberrant S1P signaling has been implicated in several chronic inflammatory and fibrotic diseases, as well as in endometriosis, but its role in adenomyosis remains poorly explored (Bernacchioni *et al.*, 2021, 2024; Zhang and Lu, 2023; Zhang *et al.*, 2023).

Here, we investigated the temporal dynamics of the S1P signaling in a murine model of adenomyosis and assessed the impact of two inhibitors acting at distinct regulatory levels. FTY720 (fingolimod), a functional antagonist of S1P receptors, which is a pro-drug that requires phosphorylation by sphingosine kinase-2 (SPHK2) to generate its biologically active form, and SKI-5C, a selective SPHK1 inhibitor. By comparing preventive (pre-lesional) and therapeutic (post-lesional) interventions, we provide the first preclinical evidence that pharmacological modulation of the S1P pathway can attenuate adenomyotic lesion progression.

Materials and methods

Animals

All animal procedures were approved by the Animal Ethics Committee of the University of Liege (approval numbers: 2387 and 2590) and conducted following ARRIVE guidelines. Female CD1 mice (Charles River Laboratories, Calco, Italy) were housed under controlled temperature (±21C) and 12-h light/dark cycle, with 3–4 animals per cage. Food and water were available *ad libitum*.

Published in : Molecular Human Reproduction (2026), vol. 32, issue 1, gaag009
doi.org/10.1093/molehr/gaag009
Status : Postprint (Author's version)

Adenomyosis induction

Adenomyosis was induced as previously described (Green *et al.*, 2005). A total of 79 neonatal CD1 females (postnatal day 1 = day of birth) received daily oral administration of tamoxifen (2.7µmol/kg, equivalent to 1mg/kg; Sigma-Aldrich, T5648, St. Louis, MO, USA) from postnatal days 2 to 5. Tamoxifen was suspended in a vehicle composed of peanut oil, lecithin, and condensed milk (2:0.2:3, v/v). The dosing volume was standardized at 5µl per gram of body weight and administered with a calibrated micropipette using a soft plastic feeding tube (Instechlabs, FTP-22-25, Plymouth Meeting, PA, USA). Control pups (n = 43) received vehicle alone. All pups remained with their dams until weaning at Day 21. In our hands, neonatal tamoxifen administration induces adenomyosis in 92–95% of CD1 females at 12weeks, consistent with previously published rates (Green *et al.*, 2005).

Experimental design and pharmacological interventions

To assess temporal S1P modulation, animals were sacrificed at 4weeks (early stage) or 12weeks (late stage) after tamoxifen/vehicle treatment.

To assess S1P inhibitors, two experimental timelines were applied. In an early intervention model (EIM), mice received daily intraperitoneal injections of FTY720 (5mg/kg in DMSO; MedChemExpress, HY-12005) or DMSO vehicle for 3 weeks starting at weaning (3weeks of age). Groups included: control (no tamoxifen), ADM+vehicle, ADM+FTY720. In the late intervention model (LIM), treatments began at 6weeks, when adenomyotic lesions were established, mice were treated daily for 3weeks with FTY720 (5mg/kg) or the SPHK1 inhibitor SKI-5C (10mg/kg; Abcam, ab144410, dissolved in methyl acetate) (Abcam, Cambridge, UK). Vehicle-treated and untreated controls were included. An exploratory cohort (n = 5–6/group) was followed by a confirmatory experiment (n = 7/group) enabling immune profiling.

Histology and immunohistochemistry

Uteri were fixed in 4% paraformaldehyde, embedded in paraffin, and sectioned at 5µm (Leica RM2125RT, Wetzlar, Germany). Sections were deparaffinized, rehydrated, and subjected to antigen retrieval (Target Retrieval Solution, Dako, S1699, Santa Clara, CA, USA, 1:10; autoclave, 126C, 1.4bar). Endogenous peroxidase was blocked with 3% H_2O_2 (1:10, Carl ROTH, 22029501, Karlsruhe, Germany) for 20min, followed by incubation in blocking buffer (Cell Signaling, 15019L, 1:5, Danvers, MA, USA).

Tissues were incubated for 1h at room temperature with primary antibodies: rabbit anti-EpCAM (1:400, Cell Signaling, 93790) to detect endometrial epithelial cells, and FITC-conjugated mouse anti-aSMA (1:400, Sigma-Aldrich, F3777) for smooth muscle cells. After PBS washes, EpCAM staining was revealed with HRP-conjugated secondary antibody (Dako ENVISION K4003, ready-to-use) for 30min and TSA-Cy3 signal amplification (1:2000, PerkinElmer, Shelton, CT, USA). Slides were counterstained with DAPI (Fluoromount-G, SouthernBiotech, Birmingham, AL, USA) and scanned using an Olympus SLIDEVIEW VS2000 microscope (Olympus, Antwerp, Belgium). $EpCAM^+$ cells appeared red and $aSMA^+$ muscle cells green.

Quantification of adenomyosis lesions

Image analysis and measurements were performed using MATLAB R2024b (MathWorks, Natick, MA, USA). Fluorescence images of the endometrium–myometrium interface were recorded in the RGB (red, green, blue) color space, with EpCAM, aSMA, and DAPI signals appearing in the red, green, and blue channels,

Published in : Molecular Human Reproduction (2026), vol. 32, issue 1, gaag009
doi.org/10.1093/molehr/gaag009
Status : Postprint (Author's version)

respectively. The RGB images were then split, and the red channel (containing only the EpCAM staining) was segmented using MATLAB's graythresh function. This allowed the generation of a binary image in which epithelial glands appear as white pixels (pixel value = 1) on a black background (pixel value = 0).

To quantify the invasion of endometrial glands into the myometrium, the endometrium–myometrium boundary was first manually delineated. The distance of each gland pixel to this boundary was then computed using MATLAB's distance function. The resulting values were used to determine the spatial distribution of glands relative to the endometrium–myometrium interface. Importantly, this method provides a quantitative assessment of glandular invasion in adenomyosis: a measurement that, to our knowledge, has not previously been described in the literature. Because glandular invasion can occur throughout the entire thickness of the myometrium, no fixed penetration limit was applied; the analysis captures the presence of EpCAM- positive glands across the full myometrial thickness.

Lesion severity was graded according to the extent of adenomyotic involvement of the inner one-third (grade I, superficial adenomyosis), two-thirds (grade II), or the entire myometrial thickness (grade III, deep adenomyosis), as previously described and illustrated (Squatrito *et al.*, 2024).

Flow cytometry analysis

Uteri were minced and digested enzymatically in Hank's balanced salt solution (HBSS) supplemented with 2.5mg/ml collagenase Type IA (Sigma-Aldrich, C9891) to obtain single-cell suspensions. After filtering, cells were washed and stained with fluorochrome-conjugated antibodies against CD45, CD11b, F4/ 80, CD86, CD163, CD3, CD4, CD8, and NKp46 (details in Table 1). Dead cells were excluded with the LIVE/DEAD Fixable Aqua reagent, and doublets were removed by FSC/SSC gating. Data were acquired on a BD FACS Aria III cell sorter (BD biosciences, San Jose, CA, USA) and analyzed with FlowJo software (version 10, BD Biosciences, Ashland, OR, USA). The gating strategy is shown in Supplementary Fig. S1. Briefly, after exclusion of doublets and dead cells, live cells were then gated for CD45 expression to define total leukocytes. Within the $CD45^+$ compartment, expression of CD11b and F4/80 was used to delineate major immune subsets. Macrophages were identified as $CD11b^+F4/80^+$ cells and further characterized by the independent expression of CD86 and CD163 as functional markers.

Table 1. Antibodies used for flow cytometry.

Marker	Clone	Fluorochrome	Supplier	City and country	Catalog no.
CD45	30-F11	PeCy7	BioLegend	San Diego, CA, USA	103114
CD3	17A2	BB700	BD Biosciences	San Jose, CA, USA	742175
CD4	GK1.5	BV711	BioLegend	San Diego, CA, USA	100447
CD8	53-6.7	APC-Cy7	BD Biosciences	San Jose, CA, USA	561967
NKp46	29A1.4	BV650	BioLegend	San Diego, CA, USA	137635
CD11b	M1/70	BV785	BioLegend	San Diego, CA, USA	101243
F4/80	BM8	BV605	BioLegend	San Diego, CA, USA	123133
CD86	GL-1	Pe-Dazzle594	BioLegend	San Diego, CA, USA	105041
CD163	S15049F	APC	BioLegend	San Diego, CA, USA	156705
Live/Dead Fixable Aqua	_	_	ThermoFisher Scientific	Waltham, MA, USA	L34957
Fc Block	2.4G2	_	BD Biosciences	San Jose, CA, USA	553142

Published in : Molecular Human Reproduction (2026), vol. 32, issue 1, gaag009
doi.org/10.1093/molehr/gaag009
Status : Postprint (Author's version)

Cells negative or low for both CD11b and F4/80 were analyzed for CD3 and CD19 expression to distinguish T cells ($CD3^+CD19^-$) and B cells ($CD3-CD19^+$). Within the CD3+ T-cell population, natural killer T (NKT)-like cells were defined as $CD3^+NKp46^+$ cells, and T cells were further subdivided based on CD4 and CD8 expression into $CD4^+$, $CD8^+$, double-negative ($CD4^-CD8^-$), and double-positive ($CD4^+CD8^+$) subsets. In parallel, NK cells were identified as $NKp46^+$ cells within the $CD45^+CD11b^+F4/80^-$ population. Compensation was verified using unstained, single-stain, and fluorescence-minus-one (FMO) controls, and intrinsic uterine autofluorescence was taken into account during gating and compensation validation.

Gene expression (RTq-PCR)

For mouse uterine horns, total RNA was isolated using RNeasy® Mini Kit (Qiagen, Hilden, Germany), following the manufacturer's protocol for tissue samples. For each sample, 1µg RNA was reverse transcribed into cDNA using FastGene Scriptase II Ready Mix (Nippon Genetics, LS64, Duren, Germany). Quantitative real- € time PCR was performed with SYBR Green PCR Master Mix (Nippon Genetics, LS4005) on a QuantStudio 3 system (Thermo Fisher Scientific, Waltham, MA, USA). Gene expression analysis focused on S1P pathway receptors and metabolic enzymes as well as *Il6*, *Tnfα*, *Il10*, *Tgfβ*, *Vegf*, and *Plau*. Expression levels were normalized to *Gapdh* and *Rplp0* (Lin *et al*., 2013). Relative expression was calculated using the 2−DCt method as recommended for comparisons across biological samples (Schmittgen and Livak, 2008). Primer sequences are listed in Table 2.

Table 2. Primers sequences used for RT-qPCR analysis of murine uterine genes.

Gene	Forward primer	Reverse primer	Amplicon size (bp)
S1pr1	CTCTTCTGCACCACCGTCTT	CGACTGGCCTTGGAGATGTT	128
S1pr2	TGTTGCTGGTCCTCAGACGCTA	AGTGGGCTTTGTAGAGGACAGG	149
S1pr3	GCCTTGCAGAACGAGAGCCTA	CTGCCAGTTTCCCCACGTAA	246
S1pr4	GTGTATGGCTGCATCGGTCTGT	GAGCACATAGCCCTTGGAGTAG	135
S1pr5	GTGTACACCAAATGCCCAGC	AGCACTGTGCAAAAGTCTCCT	101
Sphk1	GCTTCTGTCAACCACTATGCTGG	ACTGAGCACAGAATAGAGCCGC	153
Sphk2	GGTGCCAATGATCTCTGAAGCTG	CTCCAGACACAGTGACAATGCC	128
Sgpp1	CTGGAGGTCTTCTACAACTCGG	GTGAACTCCAGCAGGGAATGAG	151
Sgpp2	ATGGCTGTGTTCTCTACGC	GGTAGGTCAGAGCAATGAGGAC	115
Sgpl	GGAAAGCCTCAGGAGCTGTGTA	CTGCCTCTAACTTCCGCAATCC	132
Il6	ACCTGGAGTACATGAAGAACAACTT	GCTCTTGGTTGAAGATATGAATTAGA	102
Tnfα	TCTTCTCATTCCTGCTTGTGG	GAGGCCATTTGGGAACTTCT	106
Il10	GCTCTTACTGACTGGCATGAG	CGCAGCTCTAGGAGCATGTG	105
TGFß	CGTCACTGGAGTTGTACGGCAG	CGTTTGGGGCTGATCCCGTTG	109
Vegf	GTCCTGTGTGCCGCTGAT	AGGTTTGATCCGCATGATCT	101
Plau	AGAAGCGACCCTGGTGCTATGT	CCACACTGGAAGCCTTGTTGGT	145
Gapdh	GGTGGACCTCATGGCCTACA	CTCTCTTGCTCAGTGTCCTTGCT	82
Rplp0	GGACCCGAGAAGACCTCCTT	GCACATCACTCAGAATTTCAATGG	85

Primer design and validation

All primers were designed using NCBI Primer-BLAST to ensure target specificity and, when possible, to span exon–exon junctions. Primer specificity was verified experimentally by melt- curve analysis, which consistently showed a single amplification peak. Amplification efficiency was determined from standard curves generated using serial dilutions of pooled cDNA; only primer pairs with efficiencies between 90% and 110% and an $R^2 \geq 0.99$ were retained for analysis.

Published in : Molecular Human Reproduction (2026), vol. 32, issue 1, gaag009
doi.org/10.1093/molehr/gaag009
Status : Postprint (Author's version)

Statistical analysis

Data are presented as mean ± SEM or as median ± interquartile range (IQR), depending on data normality. For comparisons involving more than two groups, one-way ANOVA was performed using parametric or non-parametric tests according to the distribution of the data. Statistical comparisons of gland area distributions between experimental conditions were performed using the Kolmogorov–Smirnov test. A *P*-value < 0.05 was considered statistically significant. All statistical analyses were performed using GraphPad Prism software (San Diego, CA, USA). Additional details regarding the specific tests and *post hoc* analysis used are provided in the figure legends.

Results

Dynamic modulation of the S1P axis in the uterus of adenomyosis-induced mice at pre- and post-lesional stages

To investigate the potential involvement of the S1P signaling pathway in adenomyosis (ADM), we assessed the mRNA expression of S1P receptors and metabolic enzymes in the uteri of control and ADM mice at both 4 and 12weeks of age (Fig. 1A). These time points correspond to an early pre-lesional stage and a later stage with well-established lesions, as previously reported (Squatrito *et al.*, 2024).

At 4weeks, ADM mice displayed significant upregulation of *S1pr1* and *S1pr2* compared to controls (*P* = 0.0009; *P* = 0.0005, respectively), while *S1pr3* and *S1pr4* remained unchanged and *S1pr5* was undetectable. At 12weeks, *S1pr1* expression remained elevated (*P* = 0.003) and *S1pr4* became upregulated (*P* = 0.0232) in ADM mice, whereas *S1pr2* and *S1pr3* were no longer different from controls; *S1pr5* stayed undetectable (Fig. 1B).

For metabolic enzymes, *Sgpl*, mediating irreversible S1P degradation, was reduced at 4weeks in ADM mice (*P* = 0.0076), while the expression levels of *Sphk1*, *Sphk2*, *Sgpp1*, and *Sgpp2* were unchanged. At 12weeks, *Sphk1*, driving S1P synthesis, was increased (*P* = 0.0458), whereas *Sgpl*, *Sgpp1*, *Sgpp2*, and *Sphk2* remained unchanged in ADM mice (Fig. 1C).

Published in : Molecular Human Reproduction (2026), vol. 32, issue 1, gaag009
doi.org/10.1093/molehr/gaag009
Status : Postprint (Author's version)

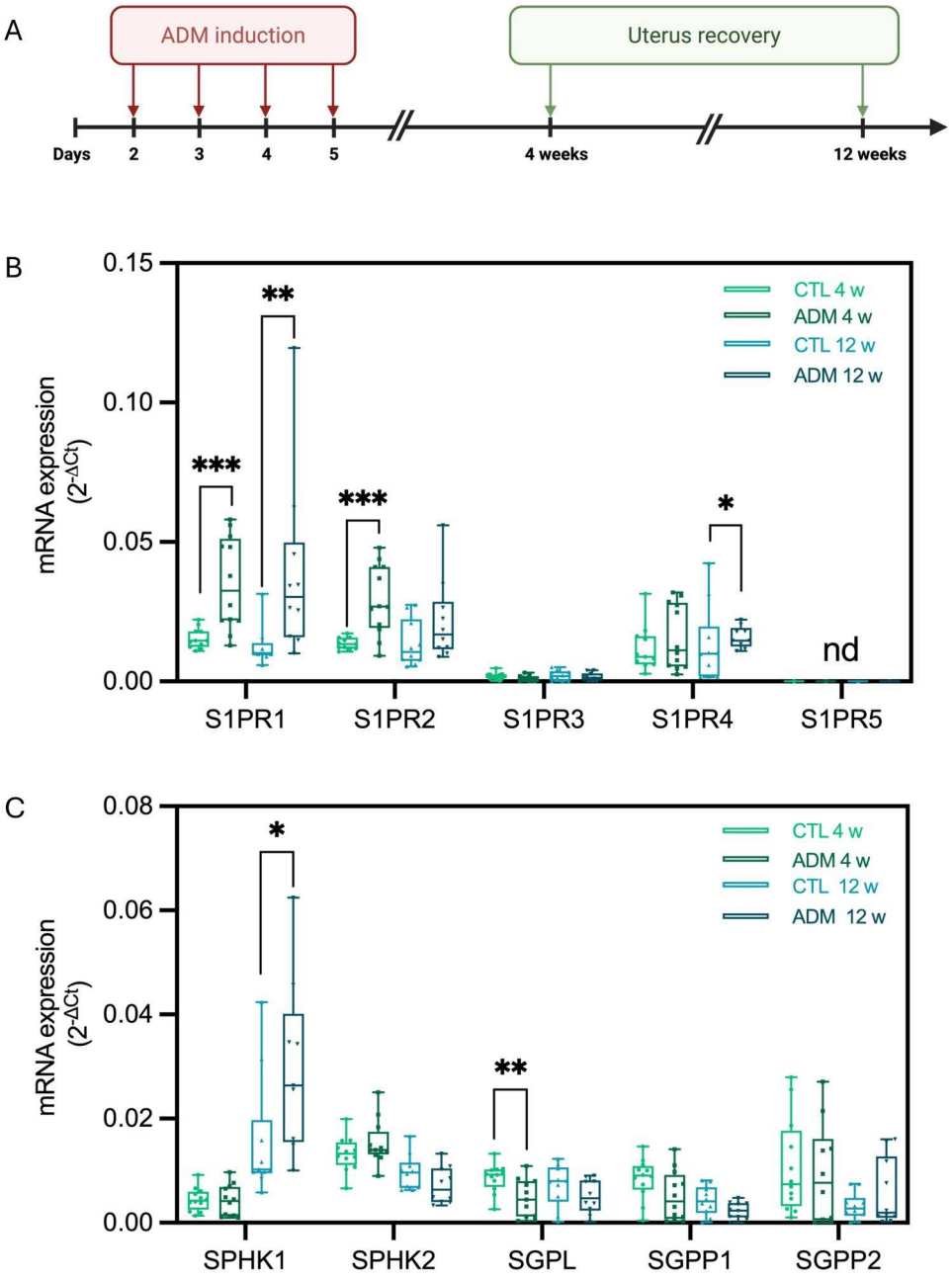

Figure 1. Stage-dependent dysregulation of the sphingosine-1-phosphate (S1P) pathway in uterine tissues from control (CTL) and adenomyosis (ADM) mice. (**A**) Experimental design for RT-qPCR analysis. (**B**) Relative mRNA expression of S1P receptors (*S1pr1–S1pr5*) at 4 and 12 weeks. (**C**) Relative expression of genes encoding S1P-metabolizing enzymes (*Sphk1*, *Sphk2*, *Sgpl*, *Sgpp1*, *Sgpp2*) at 4 and 12 weeks. At 4 weeks, adenomyotic uteri showed increased expression of *S1pr1* and *S1pr2* together with reduced *Sgpl*, whereas at 12 weeks, *S1pr1* remained elevated and *S1pr4* and *Sphk1* were upregulated, with no change in other S1P receptors or metabolic enzymes. Gene expression was normalized to the geometric mean of *Rplp0* and *Gapdh*. Data are presented as median with interquartile range (IQR). Group sizes were n = 12 mice at 4 weeks and n = 10 mice at 12 weeks. Statistical analyses were performed using parametric or non-parametric tests depending on data distribution. **P* < 0.05; ***P* < 0.01; ****P* < 0.001; nd, not detectable.

Preventive and therapeutic pharmacological modulation of the s1p pathway: effects on murine and uterine weights

Given the modulation of S1P signaling genes observed in uteri from ADM mice, we next investigated whether pharmacological inhibition could influence disease development and progression. Two *in vivo*

Published in : Molecular Human Reproduction (2026), vol. 32, issue 1, gaag009
doi.org/10.1093/molehr/gaag009
Status : Postprint (Author's version)

treatment strategies were applied (Fig. 2A). In the EIM, mice received daily FTY720 from weaning for 3 weeks, targeting the pre-lesional stage. In the LIM, designed to mimic the clinical scenario in young adult women with established disease, treatments began at 6weeks of age and included both FTY720 and the SPHK1 inhibitor SKI-5C.

As an initial step, we monitored body weight evolution and uterine weight at sacrifice to assess potential systemic and uterine effects of pharmacological modulation of the S1P pathway.

In the EIM, body weight increased similarly in CTL and ADM groups, with no effect of FTY720 (Fig. 2B, left panel). In the LIM, CTL, ADM, and SKI-5C groups exhibited similar weight gain, whereas FTY720-treated mice displayed a plateau in growth that did not reach a statistically significance difference (Fig. 2B, middle panel).

At sacrifice, uterine weight relative to body weight was lower in ADM mice than in CTL mice in both models. In the EIM, FTY720 did not modify this reduction. In the LIM, FTY720 again had no effect, whereas SKI-5C further decreased relative uterine weight compared to ADM mice (Fig. 2C). Given that uterine weight reflects both physiological myometrial growth and pathological remodeling, these changes are interpreted in conjunction with lesion prevalence and depth rather than as standalone indicators of treatment efficacy.

Although neither FTY720 nor SKI-5C restored uterine weight, we next investigated their impact on adenomyotic lesions, since lesion prevalence and severity are the main histological hallmarks of disease progression.

Impact of pharmacological modulation of the s1p pathway on adenomyosis lesion prevalence, grading, and depth

We first assessed the overall impact of pharmacological modulation of the S1P pathway on lesion prevalence and severity. Representative immunofluorescence images of uterine sections from CTL, ADM, and treated mice are shown in Fig. 2D. In the EIM, FTY720 significantly reduced lesion prevalence compared to ADM mice (Fig. 2E). In the LIM, SKI-5C markedly decreased lesion prevalence, whereas FTY720 had no effect.

Analysis of lesion grades (Fig. 2F) provided an insight into lesion severity independently of prevalence. In the EIM, FTY720 reduced the proportion of high-grade (grade 3) lesions compared to untreated ADM, indicating that preventive treatment is associated with a reduced proportion of high-grade lesions. In the LIM, no statistically significant differences in lesion grades were detected. Quantitative details of lesion prevalence and grades are provided in Supplementary Table S1.

These observations prompted a closer examination of glandular distribution within the myometrium to better characterize lesion architecture (Fig. 2G). In the EIM, gland distribution in ADM and FTY720-treated mice overlapped near the endometrial–myometrial junction, but FTY720 significantly reduced glandular area in deeper layers (P = 0.0025; Fig. 2H). In the LIM, FTY720 had no detectable effect, whereas SKI-5C markedly reduced gland area throughout the myometrium (P = 0.0005), with effects evident even close to the junction (Fig. 2I).

Published in : Molecular Human Reproduction (2026), vol. 32, issue 1, gaag009
doi.org/10.1093/molehr/gaag009
Status : Postprint (Author's version)

Modulation of uterine immune cell populations by pharmacological modulation of the S1P pathway

Previous studies in human adenomyosis and rodent models have reported alterations in macrophage infiltration and T-cell composition in the eutopic uterus (Bourdon *et al.*, 2021a, 2024; Bian *et al.*, 2025). To explore the immunomodulatory effects of targeting S1P signaling at distinct regulatory levels in our model, we analyzed uterine macrophage and T cell populations as well as B cells by flow cytometry in the LIM.

Total uterine macrophages ($CD45^+CD11b^+F4/80^+$) were modestly reduced in ADM compared to CTL mice, although this difference did not reach statistical significance (Fig. 3A). SKI-5C significantly reduced macrophage abundance compared with CTL (P = 0.025), whereas FTY720 had no effect. Macrophage polarization did not differ across groups as assessed by CD86 and CD163 expression within the $CD45^+CD11b^+F4/80^+$ population (Fig. 3B–D), indicating no major shift in these macrophage- associated functional markers across conditions. Representative flow cytometry panels illustrating macrophage gating and polarization are shown in Supplementary Fig. S2.

B cells constituted a minor fraction of uterine leukocytes and did not differ significantly between CTL, ADM, FTY720-treated or SKI-5C-treated mice (Fig. 3E).

We next examined the innate-like lymphoid population. NK- cell abundance did not differ significantly between CTL, ADM, and FTY720-treated groups. In contrast, SKI-5C treatment was associated with a significant increase in uterine NK cells compared with both ADM (P = 0.0006) and FTY720-treated mice (P = 0.0112) (Fig. 3F).

We subsequently examined the T-cell compartment. Total uterine T cells tended to be reduced in ADM mice compared with CTL mice, suggesting a modest alteration of T-cell homeostasis associated with adenomyosis. A significant decrease in total T- cell abundance was observed in FTY720-treated mice relative to CTL mice (P = 0.0365), consistent with the known lymphocyte- sequestering effects of S1P receptor modulation. In contrast, SKI- 5C-treated mice exhibited total T-cell levels comparable to those of CTL mice, indicating that sphingosine kinase inhibition preserved uterine T-cell abundance despite disease induction and pharmacological intervention (Fig. 3G). Within this T-cell compartment, NKT-like cells were significantly increased in SKI-5C- treated mice compared with CTL mice (P = 0.0054) (Fig. 3H). Evaluation of conventional T-cell subsets showed a trend toward increased $CD4^+CD8^-$ T cells in ADM mice compared with CTL, as well as a significant increase in $CD4^+CD8^-$ T cells in SKI-5C- treated mice (P = 0.02). In contrast, the abundance of $CD8^+CD4^-$ T cells did not differ significantly between the experimental groups. Similarly, no significant differences were observed for double-negative or double-positive T-cell populations across groups. Overall, double-negative T cells represented the most abundant subset in all conditions, whereas double-positive T cells remained rare (Fig. 3I). Representative flow cytometry panels of B cells, NK cells, and T-cell populations subsets are shown in Supplementary Fig. S3.

Overall, pharmacological modulation of this S1P pathway, particularly through sphingosine kinase inhibition with SKI-5C, was associated with selective alterations in uterine immune cell populations, whereas adenomyosis alone induced limited changes in the immune compartments analyzed.

Published in : Molecular Human Reproduction (2026), vol. 32, issue 1, gaag009
doi.org/10.1093/molehr/gaag009
Status : Postprint (Author's version)

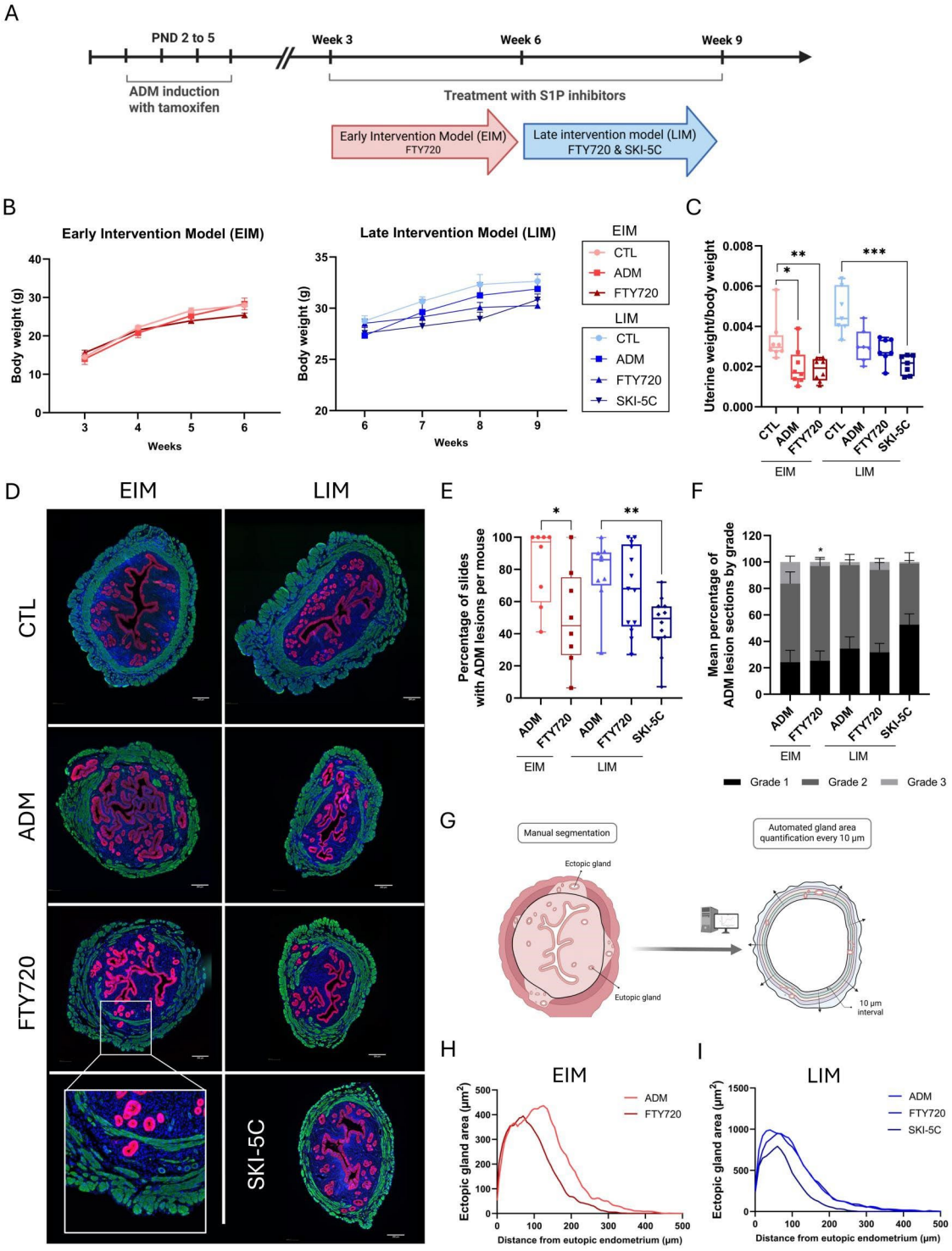

Figure 2. Preventive and therapeutic pharmacological modulation of the sphingosine-1-phosphate (S1P) pathway: systemic effects and lesion outcomes. (**A**) Experimental design: early intervention model (EIM) with daily FTY720 from weaning for 3 weeks, and late intervention model (LIM) with daily FTY720 or SKI-5C initiated at 6 weeks of age, when lesions were established. (**B**) Body weight evolution during treatment. Body-weight trajectories are shown to document potential systemic effects of FTY720 and SKI-5C during disease progression, as uterine-weight ratios can only be assessed at sacrifice. (**C**) Uterine weight at sacrifice normalized to body weight. Preventive and therapeutic pharmacological modulation of the S1P pathway did not restore uterine weight in adenomyotic (ADM) mice, although SKI-5C further reduced relative uterine weight in the late intervention model. (**D**) Representative uterine sections from control (CTL), ADM, and treated groups in EIM (FTY720) and LIM (FTY720, SKI-5C). Red highlights = epithelial glands (EpCam immunolabeling); green = myometrium (aSMA immunolabeling). Scale bar,200µm (**E**) Prevalence of adenomyotic lesions, expressed as percentage of uterine sections containing ectopic glands. An average of 19 ±

Published in : Molecular Human Reproduction (2026), vol. 32, issue 1, gaag009
doi.org/10.1093/molehr/gaag009
Status : Postprint (Author's version)

2 sections per animal (EIM) and 35 ± 4 (LIM) were analyzed spaced by ≥50 µm. (**F**) Distribution of lesion grades was defined according to adenomyotic involvement of the inner third (grade I), two-thirds (grade II), or entire myometrium (grade III). (**G**) Diagram illustrating the quantification pipeline: manual segmentation of ectopic glands and automated quantification of glandular area every 10 µm from the endometrial–myometrial junction. (**H–I**) Ectopic glandular invasion plotted as gland area versus distance from eutopic endometrium in EIM (**H**) and LIM (**I**). Preventive FTY720 treatment significantly reduced lesion prevalence, the proportion of high-grade lesions, and glandular invasion depth, whereas in established disease, only SKI-5C decreased lesion prevalence and reduced glandular invasion throughout the myometrium. Sample sizes: for body and uterine weights (B and C), n = 8 mice/group in EIM and n = 7 mice/group in LIM; for lesion prevalence and invasion analyses (E, H–I), n = 8 mice/group in EIM, and n = 9 ADM, 13 FTY720, and 12 SKI-5C in LIM. Statistical significance was determined using the Kruskal–Wallis test followed by Dunn's *post hoc* test for panels B, C, E; the Kolmogorov–Smirnov test for panels H and I; the Kruskal–Wallis test for the analysis of lesion grades in the LIM group; and the Mann– Whitney *U* test in the EIM group for Panel F. **P* < 0.05; ***P* < 0.01; ****P* < 0.001.

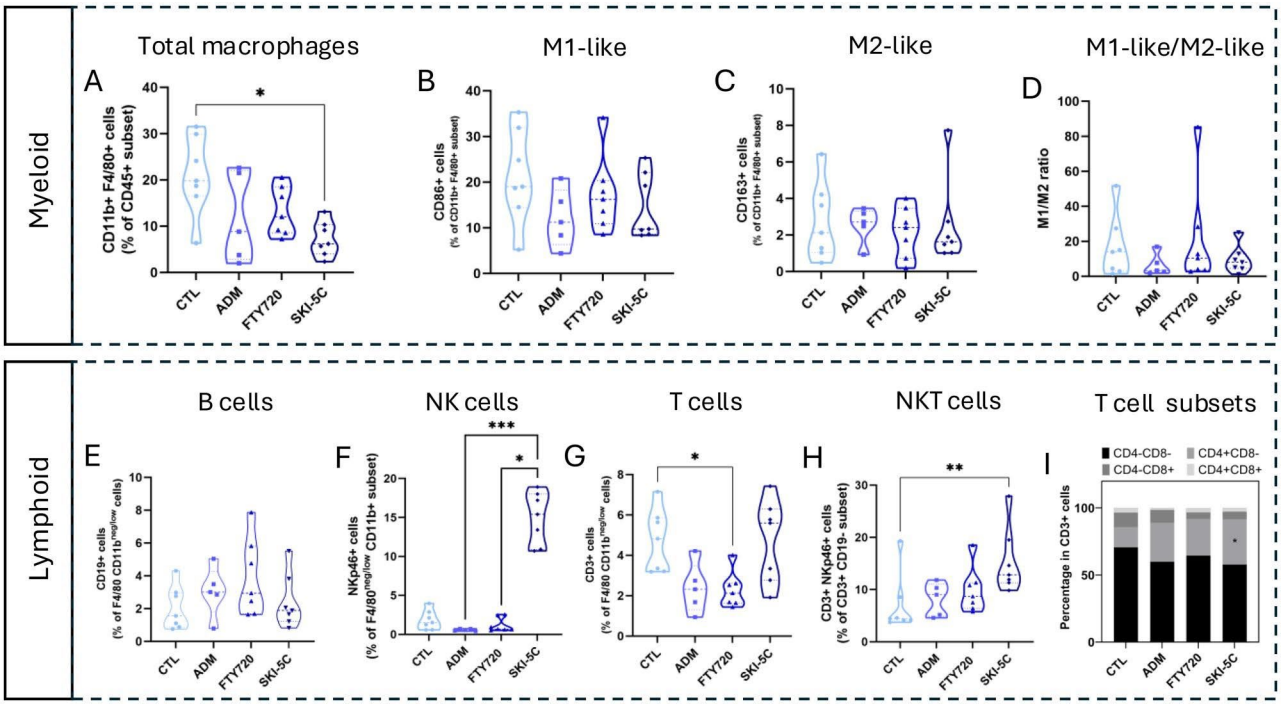

Figure 3. Immune profiling of adenomyosis following sphingosine-1-phosphate (S1P) pathway inhibition. Representative violin plots showing the percentage of (**A**) total macrophages ($CD45^+F4/80^+CD11b^+$), (**B**) M1-like macrophages ($F4/80^+CD11b^+CD86^+$), (**C**) M2-like macrophages ($F4/80^+CD11b^+CD163^+$), (**D**) M1-like/M2-like macrophages ratio, (**E**) B cells ($CD45^+F4/80^{low/neg}CD11^{low/neg}CD19^+$), (**F**) NK cells ($CD45^+F4/80^{low/neg}CD11b^+NKp46^+$), (**G**) total T cells ($CD45^+F4/80^{low/neg}CD11^{low/neg}CD3^+$), (**H**) NKT-like cells ($CD3^+NKp46^+$), and (**I**) T cells subsets: $CD4^-CD8^-$ (DN, black), $CD4^+CD8^-$ ($CD4^+$, light grey), $CD4^-CD8^+$ ($CD8^+$, dark grey), and $CD4^+CD8^+$ (DP, very light grey), in uteri of control (CTL), adenomyosis (ADM), and treated (FTY720 and SKI-5C) mice. Rows correspond respectively to CTL, ADM, FTY720, SKI-5C. The late intervention model revealed no major immune alterations associated with adenomyosis alone, with unchanged macrophage polarization and B-cell abundance. In contrast, SKI-5C selectively modulated uterine lymphoid populations by increasing NK and NKT- like cells and preserving total T-cell levels, whereas FTY70 reduced uterine T-cell abundance. Group sizes were n = 7. Statistical significance was determined using the Kruskal–Wallis test followed by Dunn's *post hoc* test. *P* < 0.05; *P* < 0.01.

Modulation of inflammatory, angiogenic, and invasive gene expression by S1P inhibitorS

Given the central role of S1P signaling in inflammation, angiogenesis, and tissue remodeling, we next explored whether pharmacological inhibition modulates the uterine expression of selected genes involved in these processes (Spiegel and Milstien, 2011; Donati *et al.*, 2021; Gomez-Larrauri *et al.*, 2025). We focused on cytokines with pro-inflammatory (*Il6*, *Tnfα*) or anti- inflammatory/immunoregulatory (*Il10*, *Tgfβ*) functions, the angiogenic factor *Vegf*, and the invasion-associated protease urokinase-type plasminogen

Published in : Molecular Human Reproduction (2026), vol. 32, issue 1, gaag009
doi.org/10.1093/molehr/gaag009
Status : Postprint (Author's version)

activator (*Plau*), comparing expression patterns across CTL, ADM, and treated groups in both intervention models (EIM and LIM).

In ADM mice, *Il6* expression was significantly increased in the EIM ($P = 0.0479$), and FTY720 treatment did not counteract this increase. In the LIM, *Il6* did not differ between CTL and ADM, but both inhibitors induced *Il6* upregulation compared to CTL ($P<0.01$, Fig. 4A). *Tnfa* remained unchanged between CTL and ADM in both models, and neither inhibitor modified *Tnfa* levels relative to ADM (Fig. 4B). *Il10* expression was increased by FTY720 in the EIM ($P = 0.0486$, FTY720 vs CTL) and by both inhibitors in the LIM ($P<0.001$; Fig. 4C). *Tgfb* did not differ markedly between CTL and ADM in either model. Neither FTY720 nor SKI-5C significantly modified *Tgfb* expression compared with ADM in the EIM or LIM (Fig. 4D). The apparent reductions observed in both models occur only when treatments are compared with CTL ($P < 0.05$), a comparison that is not biologically informative in this context. *Vegf* expression was significantly lower in ADM mice compared to CTL in the EIM ($P = 0.0497$) and remained low in FTY720 treated mice ($P = 0.05$; Fig. 4E). In the LIM, *Vegf* expression in ADM uteri was comparable to CTL, whereas both FTY720 and SKI-5C significantly decreased *Vegf* compared with CTL (FTY720 $P = 0.0036$ and SKI-5C $P = 0.0051$), without significant differences relative to ADM (Fig. 4E). Finally, *Plau* expression tended to be elevated in ADM mice, but this increase was not statistically significant, and levels were normalized by both inhibitors in the LIM (ADM vs FTY720 $P = 0.0066$; ADM vs SKI-5C $P = 0.003$; Fig. 4F).

Overall, targeting S1P signaling at distinct regulatory levels variably affected inflammatory cytokines, consistently suppressed *Vegf* in treated groups, and robustly normalized *Plau*, indicating convergent effects on angiogenic and invasive-associated readouts, which complement the histological readouts.

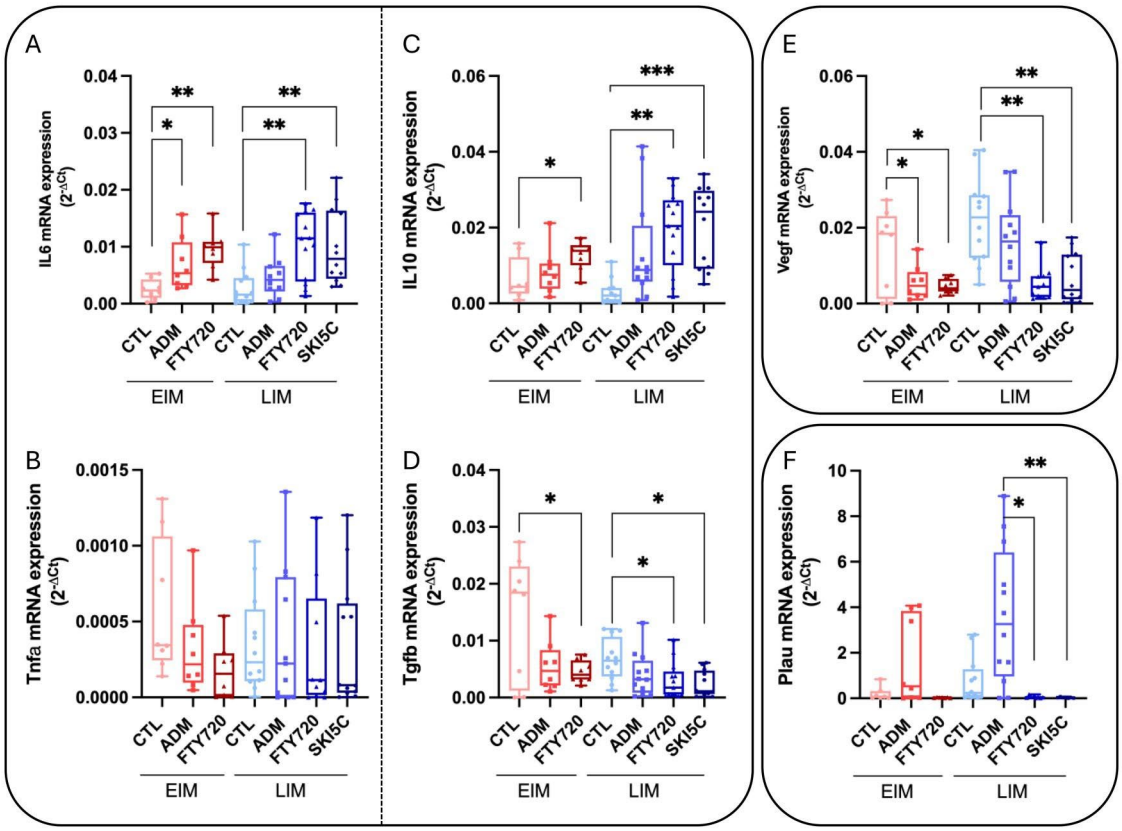

Figure 4. Modulation of inflammatory, angiogenic, and invasive gene expression in uterine tissues following sphingosine-1-phosphate (S1P) pathway inhibition in early (EIM) and late (LIM) intervention models. (**A** and **B**) Relative mRNA expression of inflammatory (*Il6*, *Tnfα*) and (**C** and **D**) regulatory (*Il10*, *Tgfβ*) cytokines, as well as (**E**) angiogenic (*Vegf*) and (**F**) invasive (*Plau*)

mediators. Expression was normalized to *Gapdh* and *Rplp0*. Data are presented as median with interquartile range (IQR). Pharmacological modulation of the S1P pathway variably affected inflammatory cytokine gene expression, with both FTY720 and SKI-5C decreasing *Vegf* expression and normalizing *Plau* levels, indicating convergent effects on angiogenic and invasion-related pathways that parallel the histological findings. Sample sizes: n = 8 mice/group in EIM and n = 12 CTL, n = 9 ADM, n = 13 FTY720, and n = 12 SKI-5C in LIM. Statistical significance was determined using the Kruskal–Wallis test with Dunn's *post hoc* correction. $*P < 0.05$; $**P < 0.01$; $***P < 0.001$.

Discussion

Our study provides evidence for a dynamic, stage-dependent dysregulation of the S1P signaling pathway in a murine model of adenomyosis and evaluates the therapeutic potential of targeting this pathway with two pharmacological inhibitors, FTY720 and SKI-5C. By integrating gene expression analysis, histological assessment, and immune profiling, we demonstrated that pharmacological inhibition of S1P signaling modulates lesion burden and invasion depth and is associated with changes in immune cell composition and selected inflammatory and angiogenic transcripts such as *Vegf* and *Plau*. The rationale for focusing on the S1P pathway stems from its established role in inflammation, fibrosis, angiogenesis, and immune cell trafficking: processes that are central to the adenomyosis pathogenesis (Spiegel and Milstien, 2011; Donati *et al.*, 2021; Gomez-Larrauri *et al.*, 2025). Importantly, our study design captured potential temporal differences in S1P signaling by analyzing both early and late disease stages and linking these findings to therapeutic interventions.

Our data support a temporal modulation of S1P pathway components, with early disease showing reduced expression of degradation enzymes and later stage marked by sustained *Sphk1* upregulation, consistent with increased S1P synthetic capacity rather than direct ligand quantification. *S1pr1* remains persistently upregulated across phases. These findings align with human data reporting altered S1P receptor expression in adenomyotic tissue, including increased *S1pr3*, decreased *S1pr2*, and correlation with the fibrosis marker ACTA2 (Vannuzzi *et al.*, 2022), as well as in endometriotic cysts and peritoneal fluid, positioning S1P as an important regulator of inflammation and angiogenesis (Santulli *et al.*, 2012; Bernacchioni *et al.*, 2021, 2024; Zhang and Lu, 2023). Beyond uterine pathology, S1P signaling has well- established roles in vascular and immune regulation. S1PR1 regulates lymphocyte trafficking and vascular integrity through mechanisms involving VE-cadherin and VEGFR2 (Gaengel *et al.*, 2012), reinforcing its relevance as a therapeutic target in adenomyosis.

This stage-dependent hypothesis is directly supported by our pharmacological experiments. FTY720 was effective only in early disease, whereas SKI-5C exerted significant effects in established lesions, consistent with their distinct modes of action and with the stage-specific expression patterns observed *in vivo*. It is important to note that FTY720 (fingolimod) is a pro-drug that requires phosphorylation by sphingosine kinase-2 (SPHK2) to generate FTY720-phosphate, which induces internalization and degradation of S1PR1, S1PR3, S1PR4, and S1PR5 while sparing S1PR2 (Brinkmann *et al.*, 2002). These pharmacological properties provide a plausible framework to interpret the observation that receptor functional antagonism and synthesis inhibition display efficacy at different stages of the disease, without implying differences in ligand availability. Similar effects have been reported in endometriosis models, where FTY720 reduced inflammation and fibrosis and SKI-5C inhibited lesion growth and vascularization (Rudzitis-Auth *et al.*, 2021; Zhang *et al.*, 2023). Although relative uterine weight was reduced in ADM groups compared with CTL mice in EIM, neither FTY720 in the EIM nor both inhibitors in the LIM significantly modified this parameter

compared with untreated ADM. In the neonatal tamoxifen model, decreased uterine weight mainly reflects myometrial remodeling rather than lesion burden, and we therefore considered it as a non- specific structural read-out rather than a prognostic marker. The absence of uterine weight normalization despite clear effects on lesion prevalence and invasion further supports the notion that S1P pathway modulation primarily targets lesion biology rather than reversing established myometrial architecture. Accordingly, uterine weight changes should not be overinterpreted, and a more refined assessment of myometrial architecture would be required to determine whether SPHK1 inhibition could influence this parameter.

Our findings indicate that S1P dysregulation contributes to the altered immune landscape of adenomyosis. SKI-5C significantly reduced macrophage abundance compared with CTL, whereas macrophage levels in ADM were not significantly altered by treatment. Macrophage polarization markers remained unchanged across groups in our model. This profile differs from some reports in human studies emphasizing M2-like dominance as a key mediator of invasion, fibrosis, and epithelial-to- mesenchymal transistion in ADM and endometriosis (Bourdon *et al.*, 2021b; Stratopoulou *et al.*, 2023; Qiu *et al.*, 2024). In line with the view that the classical M1/M2 paradigm is overly simplistic (Nahrendorf and Swirski, 2016), CD86 and CD163 in our study were therefore interpreted as proxy markers of pro- inflammatory/antigen-presenting versus more tolerogenic/ tissue-repair oriented programs, rather than as strict M1/M2 lineages. It is therefore conceivable, based on previous studies, that macrophages may play a more prominent role during the early phases of the disease; however, this was not directly addressed in the present late-stage model.

In contrast, adaptive immunity appeared more dynamically modulated. In our model, total T-cell abundance showed only limited changes in adenomyotic uteri, with a non-significant decrease compared with controls. FTY720 treatment was associated with a significant reduction in total T cells, consistent with its known effects on lymphocyte trafficking. In contrast, SKI-5C- treated mice exhibited same levels of T cells as controls, suggesting a distinct impact on lymphoid homeostasis.

Pharmacological modulation of the S1P pathway further influenced T-cell composition. While $CD4^+$ T cells tended to be increased in ADM mice, this difference did not reach statistical significance, suggesting that alterations in helper T-cell representation may be subtle at this stage of disease progression. These findings partially align with reports of $CD4^+$ T cells predominance and Th17/Treg imbalance in patients (Gui *et al.*, 2014; Lin *et al.*, 2022). $CD8^+$ cytotoxic T cells remained unchanged, which does not support a major contribution of $CD8^+$ cytotoxic responses in this model of disease progression (Liu *et al.*, 2022). A particularly intriguing finding was the SKI-5C-induced increase in NK cells as well as in NKT cells. NKT cells are a heterogeneous lymphocyte population known to exert immunomodulatory functions in various inflammatory and autoimmune contexts (Marrero *et al.*, 2015; Ahmadi *et al.*, 2022). However, their specific role in adenomyosis has not been defined. The increase in NK and NKT-like cells following SKI-5C treatment therefore reflects a treatment-associated shift in lymphoid composition rather than immune normalization. In the absence of functional or lineage-specific analyses, no conclusion can be drawn regarding their contribution to inflammation control or disease resolution in this model.

Across all experimental groups, double-negative ($CD4^-CD8^-$) T cells constituted the predominant T-cell subset in the uterine compartment. This compartment has been reported to include a significant proportion of γδ T cells, which represents a major lymphocyte subset in the murine uterus (Kang *et al.*, 2020; Foyle and Robertson, 2024). These cells regulate inflammation, tissue surveillance, and tissue repair through hormone-sensitive mechanisms (Kang *et al.*, 2020; Pawłowska *et al.*, 2022; Foyle and Robertson, 2024). Within this overall distribution, SKI-5C treatment was associated with an increase in $CD4^+CD8^-$ helper T cells. Collectively, these findings suggest that SKI-5C is associated with measurable changes in uterine T cell

composition. Whether these changes are functionally immunoregulatory or directly contribute to disease attenuation cannot be determined from the present data.

Cytokine profiling revealed that *Il6* was elevated in ADM, while *Il10* changes were treatment dependent. These alterations indicate a shift in inflammatory signaling but do not define a consistent pro-inflammatory signature linked to $CD4^+$ T cell accumulation. S1P–S1PR1/3 signaling can induce IL6 via ERK5 activation in endometrial stromal cells (Seidita *et al.*, 2023), and S1P has been shown to promote IL6 expression and proliferation in endometriotic cells (Yoshino *et al.*, 2019). Strikingly, pharmacological modulation of the S1P pathway increased IL10 and IL6 expression in both models. As these changes did not mirror ADM-associated alterations, they are unlikely to reflect a reversal of disease-driven cytokine dysregulation. In parallel, *Vegf* was unexpectedly reduced or unchanged in ADM in both models, despite *S1pr1* overexpression, possibly reflecting compensatory or hormonal regulation (Jung *et al.*, 2012; Bouquerel *et al.*, 2016; Cartier and Hla, 2019). FTY720 significantly reduced *Vegf* expression in both models, while SKI-5C decreased *Vegf* only relative to CTL. These changes suggest that S1P modulation can influence angiogenic signaling, although the relevance to ADM-associated alterations remains limited. Given the known role of S1PR1 in maintaining vascular integrity and regulating angiogenesis through VE-cadherin and VEGFR2 (Gaengel *et al.*, 2012), the observed transcriptional changes suggest that targeting S1P signaling may alter angiogenic and immune-related pathways. Nonetheless, additional studies will be required to confirm whether these changes impact vascular remodeling or immune cell recruitment *in vivo* (Kono *et al.*, 2004; Gaengel *et al.*, 2012).

Beyond these processes, S1P also governs the invasive behavior of endometrial cells through modulation of proteolytic activity. In our model, *Plau* expression was elevated in ADM, consistent with its known role in extracellular matrix degradation. Both FTY720 and SKI-5C normalized *Plau* levels in LIM, pointing to a shared anti- invasive effect. This aligns with the reduced lesion depth under SKI-5C and preventive FTY720. Taken together, these findings indicate that *Plau* may participate in S1P-related invasive programs, although additional pathways are likely involved (Kono *et al.*, 2004; Huang *et al.*, 2017; Fu *et al.*, 2021; Yang *et al.*, 2021).

Strengths and limitations

A major strength of our study lies in its integrative design, combining a stage-dependent murine model of adenomyosis with two pharmacological inhibitors acting through distinct mechanisms. This approach allowed us to capture the temporal evolution of S1P signaling, from early receptor-driven to later synthesis-driven alterations, and to identify stage-specific therapeutic vulnerabilities. Another strength is the integration of transcriptomic, histological, and immunological analyses, which linked molecular dysregulation to immune remodeling and lesion invasion.

Nevertheless, several limitations should be acknowledged. First, the murine model, while highly informative for dissecting temporal and mechanistic dynamics, does not fully replicate the complexity and chronicity of human adenomyosis, which develops over years and under cyclical hormonal influences. Second, immunological profiling focused on selected macrophage and T cell subsets, leaving other innate and adaptative immune cells compartments unexplored. Furthermore, the low absolute number of $CD45^+$ leukocytes acquired per sample limited the resolution of our flow-cytometric analyses, particularly for rare subsets. Future studies specifically designed to increase the number of $CD45^+$ events per sample will be required to perform more detailed stratification of uterine immune cell populations. Given the already low number of immune cells in late-stage uteri, immune profiling at early stage was not feasible due to even

lower cellularity. Third, in the EIM, no SKI-5C group was included. This choice reflected the molecular profile at 4weeks, where *Sphk1* expression was not yet increased; however, because *S1pr2* is already upregulated early and is not antagonized by FTY720, early SPHK1 inhibition may also be relevant, and the absence of both an early SKI-5C arm and an S1PR2-targeted intervention represents a limitation of the present study. Fourth, pharmacological treatments were of relatively short duration and long-term effects, recurrence, and systemic consequences were not assessed.

Another important limitation relates to the interpretation of gene expression data. Gene expression analyses were performed on whole-uterus lysates, reflecting averages expression across the tissue rather than lesion-specific changes. Because lesion incidence and severity vary between animals in this model, this approach does not allow precise determination of the contribution of lesion-bearing regions.

Protein-level mapping of S1P receptors or SPHK1 was not performed. Available antibodies lack the specificity required for reliable immunohistochemistry in uterine tissues, and Western blotting of whole-uterus lysates would not allow lesion-specific resolution in this diffuse model. For these reasons, we relied on transcript-level profiling, which provided robust comparative information despite these methodological constraints.

In addition, S1P levels were not quantified by LC–MS/MS, which will be required in future studies to directly validate the biochemical impact of pathway modulation. Lastly, translation to the clinical setting will require careful patient stratification according to disease stage, which will be a challenge given the current limitations in diagnostic tools. Together, these limitations highlight the need for validations in human tissues, broader immune and cytokine profiling, and studies addressing combinatorial and long-term treatment strategies.

Conclusion

S1P signaling is dynamically dysregulated in adenomyosis, with early receptor-driven and later synthesis-driven abnormalities. Pharmacological inhibition attenuates disease severity in a stage- dependent manner, with FTY720 being more effective pre-lesion and SKI-5C more effective post-lesion development, without restoring uterine weight. Together, our data identify S1P signaling as a stage-dependent regulator of adenomyosis progression and indicate that distinct levels of pathway targeting, i.e. receptor modulation versus synthesis inhibition, may be required at different disease phases. While these findings provide a strong preclinical rationale for S1P-directed interventions, their translational relevance will depend on precise disease staging and validation in human tissues.

Supplementary data

Supplementary data are available at *Molecular Human Reproduction* online.

Data availability

The data underlying this article will be shared on reasonable request to the corresponding author.

Acknowledgements

We gratefully acknowledge Prof. Michelle Nisolle for her support at the outset of this project, particularly in helping to secure the initial funding. The authors thank Prof. Jacques Donnez for his scientific input during discussions and Emilie Feyereisen and Isabelle Dasoul for their excellent technical assistance. We are furthermore grateful to the GIGA Flow cytometry Platform (University of Liège) for their expertise and support in cell phenotyping.

Authors' roles

Conceptualization, C.M. and M.S.; methodology, M.S., C.M., and S.B.; validation, M.S., J.V., and C.M.; formal analysis, M.S., S.B., L. B., and C.M.; investigation, M.S. and J.V. resources, M.S., J.V., S.B., L.B., and C.M., writing of original draft, M.S. and C.M.; review and editing, M.S., C.M., J.V., L.B. M.-M.D., and A.C.; supervision, C.M., project administration, C.M., A.C.; funding acquisition, C.M., A.C. All authors have read and agreed to the published version of the manuscript.

Funding

This research was funded by the Fonds de la Recherche Scientifique (F.R.S.-FNRS, Belgium), grant numbers T.0171.21, J.0169.25, F 5/4/130/5 (awarded to J.V.) and F 5/4/150/5 (awarded to M.-M.D.), the Fondation contre le Cancer grant number 2018- 072 (awarded to A.C.), and the Foundation Léon Fredericq (University of Liege), grant numbers 2023-016 and 2024-085.

Conflict of interest

The authors declare no conflict of interest. The funders had no role in the design of the study, in the collection, analyses or interpretation of data, in the writing of the manuscript, or in the decision to publish the results.

References

Abbott JA. Adenomyosis and Abnormal Uterine Bleeding (AUB-A)— pathogenesis, diagnosis, and management. *Best Pract Res Clin Obstet Gynaecol* 2017;**40**:68–81.

Ahmadi A, Fallah Vastani Z, Abounoori M, Azizi M, Labani-Motlagh A, Mami S, Mami S. The role of NK and NKT cells in the pathogenesis and improvement of multiple sclerosis following disease- modifying therapies. *Health Sci Rep* 2022;**5**:e489.

Bernacchioni C, Capezzuoli T, Vannuzzi V, Malentacchi F, Castiglione F, Cencetti F, Ceccaroni M, Donati C, Bruni P, Petraglia F. Sphingosine 1-phosphate receptors are dysregulated in endometriosis: possible implication in transforming growth factor β–induced fibrosis. *Fertil Steril* 2021;**115**:501–511.

Bernacchioni C, Rossi M, Vannuzzi V, Prisinzano M, Seidita I, Raeispour M, Muccilli A, Castiglione F, Bruni P, Petraglia F *et al.* Sphingosine-1-phosphate receptor 3 is a non-hormonal target to counteract endometriosis-associated fibrosis. *Fertil Steril* 2024; **121**:631–641.

Bian X, Sun Z, Lai J, Li B, Dong X, Guan H, Vankelecom H, Sun Y. Metabolic reprogramming and M2 macrophage depletion define the microenvironment of adenomyosis. *Front Endocrinol (Lausanne)* 2025;**16**:1602814.

Bird CC, McElin TW, Manalo-Estrella P. The elusive adenomyosis of the uterus-revisited. *Am J Obstet Gynecol* 1972;**112**:583–593.

Bouquerel P, Gstalder C, Müller D, Laurent J, Brizuela L, Sabbadini € RA, Malavaud B, Pyronnet S, Martineau Y, Ader I *et al.* Essential role for SphK1/S1P signaling to regulate hypoxia-inducible factor 2α expression and activity in cancer. *Oncogenesis* 2016;**5**:e209.

Bourdon M, Maget AS, Jeljeli M, Doridot L, Marcellin L, Thomas M, Chene C, Chouzenoux S, Batteux F, Chapron C *et al.* Reduced fertility in an adenomyosis mouse model is associated with an altered immune profile in the uterus during the implantation period. *Hum Reprod* 2024;**39**:119–129.

Bourdon M, Santulli P, Doridot L, Jeljeli M, Chene C, Chouzenoux S, ^ Nicco C, Marcellin L, Chapron C, Batteux F. Immune cells and Notch1 signaling appear to drive the epithelial to mesenchymal transition in the development of adenomyosis in mice. *Mol Hum Reprod* 2021a;**27**:gaab053.

Bourdon M, Santulli P, Jeljeli M, Vannuccini S, Marcellin L, Doridot L, Petraglia F, Batteux F, Chapron C. Immunological changes associated with adenomyosis: a systematic review. *Hum Reprod Update* 2021b;**27**:108–129.

Brinkmann V, Davis MD, Heise CE, Albert R, Cottens S, Hof R, Bruns C, Prieschl E, Baumruker T, Hiestand P *et al.* The immune modulator FTY720 targets sphingosine 1-phosphate receptors. *J Biol Chem* 2002;**277**:21453–21457.

Cartier A, Hla T. Sphingosine 1-phosphate: lipid signaling in pathology and therapy. *Science* 2019;**366**:eaar5551.

Di Paolo A, Vignini A, Alia S, Membrino V, Delli Carpini G, Giannella L, Ciavattini A. Pathogenic role of the sphingosine 1-phosphate (S1P) pathway in common gynecologic disorders (GDs): a possible novel therapeutic target. *Int J Mol Sci* 2022;**23**:13538.

Donati C, Cencetti F, Bernacchioni C, Vannuzzi V, Bruni P. Role of sphingosine 1-phosphate signalling in tissue fibrosis. *Cell Signal* 2021;**78**:109861.

Foyle KL, Robertson SA. Gamma delta (γδ) T cells in the female reproductive tract: active participants or indifferent bystanders in reproductive success? *Discov Immunol* 2024;**3**:kyae004.

Fu X, Yao M, Ye C, Fang T, Wu R. Osteopontin regulates endometrial stromal cell migration in endometriosis through the PI3K pathway osteopontin regulates endometrial cell migration in endometriosis. *Reprod Sci* 2021;**28**:435–446.

Gaengel K, Niaudet C, Hagikura K, Lavina B, Muhl L, Hofmann JJ, ~ Ebarasi L, Nystrom S, Rymo S, Chen LL € *et al.* The sphingosine-1- phosphate receptor S1PR1 restricts sprouting angiogenesis by regulating the interplay between VE-cadherin and VEGFR2. *Dev Cell* 2012;**23**:587–599.

Gomez-Larrauri A, Larrea-Sebal A, Martın C, Gomez-Munoz A. The ~ critical roles of bioactive sphingolipids in inflammation. *J Biol Chem* 2025;**301**:110475.

Green AR, Styles JA, Parrott EL, Gray D, Edwards RE, Smith AG, Gant TW, Greaves P, Al-Azzawi F, White INH. Neonatal tamoxifen treatment of mice leads to adenomyosis but not uterine cancer. *Exp Toxicol Pathol* 2005;**56**:255–263.

Gui T, Chen C, Zhang Z, Tang W, Qian R, Ma X, Cao P, Wan G. The disturbance of TH17-Treg cell balance in adenomyosis. *Fertil Steril* 2014;**101**:506–514.

Huang W, Jin A, Zhang J, Wang C, Tsang LL, Cai Z, Zhou X, Chen H, Chan HC. Upregulation of CFTR in patients with endometriosis and its involvement in NFκB-uPAR dependent cell migration. *Oncotarget* 2017;Mar 22**8**:66951–66959.

Jung B, Obinata H, Galvani S, Mendelson K, Ding BS, Skoura A, Kinzel B, Brinkmann V, Rafii S, Evans T *et al.* Flow-regulated endothelial S1P receptor-1 signaling sustains vascular development. *Dev Cell* 2012;**23**:600–610.

Kang S, Wu Q, Huang J, Yang B, Liang C, Chi P, Wu C. Tissue resident memory γδT cells in murine uterus expressed high levels of IL-17 promoting the invasion of trophocytes. *Front Immunol* 2020;**11**:588227.

Kono M, Mi Y, Liu Y, Sasaki T, Allende ML, Wu YP, Yamashita T, Proia RL. The sphingosine-1-phosphate receptors S1P1, S1P2, and S1P3 function coordinately during embryonic angiogenesis. *J Biol Chem* 2004;**279**:29367–29373.

Lin P, Lan X, Chen F, Yang Y, Jin Y, Wang A. Reference gene selection for real-time quantitative PCR analysis of the mouse uterus in the peri-implantation period. *PLoS One* 2013;**8**:e62462.

Lin J, Liu L, Zheng F, Chen S, Yang W, Li J, Mo S, Zeng DY. Exploration the global single-cell ecological landscape of adenomyosis-related cell clusters by single-cell RNA sequencing. *Front Genet* 2022;**13**:1020757.

Liu D, Yin X, Guan X, Li K. Bioinformatic analysis and machine learning to identify the diagnostic biomarkers and immune infiltration in adenomyosis. *Front Genet* 2022;**13**:1082709.

Liu Z, Sun Z, Liu H, Niu W, Wang X, Liang N, Wang X, Wang Y, Shi Y, Xu L *et al.* Single-cell transcriptomic analysis of eutopic endometrium and ectopic lesions of adenomyosis. *Cell Biosci* 2021;**11**:51.

Loring M, Chen TY, Isaacson KB. A systematic review of adenomyosis: it is time to reassess what we thought we knew about the disease. *J Minim Invasive Gynecol* 2021;**28**:644–655.

Maceyka M, Harikumar KB, Milstien S, Spiegel S. Sphingosine-1- phosphate signaling and its role in disease. *Trends Cell Biol* 2012; **22**:50–60.

Marrero I, Ware R, Kumar V. Type II NKT cells in inflammation, autoimmunity, microbial immunity, and cancer. *Front Immunol* 2015; **6**:316.

Moawad G, Fruscalzo A, Youssef Y, Kheil M, Tawil T, Nehme J, Pirtea P, Guani B, Afaneh H, Ayoubi JM *et al.* Adenomyosis: an updated review on diagnosis and classification. *J Clin Med* 2023;**12**:4828.

Nahrendorf M, Swirski FK. Abandoning M1/M2 for a network model of macrophage function. *Circ Res* 2016;**119**:414–417.

Pawłowska A, Natochina Y, Zardzewiały W, Skiba W, Włodarczyk K, Maciejczyk A, Suszczyk D, Wertel I. γδ T lymphocytes as a double-edged sword—state of the art in gynecological diseases. *Int J Mol Sci* 2022;**23**:14797.

Qiu Y, Cao J, Li S, Liu Y, Wan G, Gui T. Macrophage polarization in adenomyosis: a review. *Am J Reprod Immunol* 2024;**91**:e13841.

Rudzitis-Auth J, Christoffel A, Menger MD, Laschke MW. Targeting sphingosine kinase-1 with the low MW inhibitor SKI-5C suppresses the development of endometriotic lesions in mice. *Br J Pharmacol* 2021;**178**:4104–4118.

Santulli P, Marcellin L, Noel € JC, Borghese B, Fayt I, Vaiman D, Chapron C, Mehats C. Sphingosine pathway deregulation in endometriotic tissues. *Fertil Steril* 2012;**97**:904–911.

Schmittgen TD, Livak KJ. Analyzing real-time PCR data by the comparative CT method. *Nat Protoc* 2008;**3**:1101–1108.

Seidita I, Tusa I, Prisinzano M, Menconi A, Cencetti F, Vannuccini S, Castiglione F, Bruni P, Petraglia F, Bernacchioni C *et al.* Sphingosine 1-phosphate elicits a ROS-mediated proinflammatory response in human endometrial stromal cells via ERK5 activation. *FASEB J* 2023;**37**:e23061.

Sharara FI, Kheil MH, Feki A, Rahman S, Klebanoff JS, Ayoubi JM, Moawad GN. Current and prospective treatment of adenomyosis. *J Clin Med* 2021;**10**:3410.

Spiegel S, Milstien S. The outs and the ins of sphingosine-1- phosphate in immunity. *Nat Rev Immunol* 2011;**11**:403–415.

Squatrito M, Vervier J, Bernet L, Camboni A, Dolmans MM, Munaut C. Temporal dynamics of uterine immune microenvironment remodeling in a murine model of adenomyosis. *Mol Hum Reprod* 2025;**31**:2025. gaaf057.

Squatrito M, Vervier J, Bindels J, Bernet L, Blacher S, Nisolle M, Munaut C. Impaired fertility in adenomyosis: a murine model reveals endometrial receptivity and progesterone resistance imbalances. *Reproduction* 2024;**167**:e240019.

Stratopoulou CA, Cussac S, d'Argent M, Donnez J, Dolmans M-M. M2 macrophages enhance endometrial cell invasiveness by promoting collective cell migration in uterine adenomyosis. *Reprod Biomed Online* 2023;**46**:729–738.

Vannuccini S, Luisi S, Tosti C, Sorbi F, Petraglia F. Role of medical therapy in the management of uterine adenomyosis. *Fertil Steril* 2018;**109**:398–405.

Vannuccini S, Petraglia F. Recent advances in understanding and managing adenomyosis. *F1000Res* 2019;**8**:F1000 Faculty Rev-283.

Vannuccini S, Tosti C, Carmona F, Huang SJ, Chapron C, Guo SW, Petraglia F. Pathogenesis of adenomyosis: an update on molecular mechanisms. *Reprod Biomed Online* 2017;**35**:592–601.

Vannuzzi V, Bernacchioni C, Muccilli A, Castiglione F, Nozzoli F, Vannuccini S, Capezzuoli T, Ceccaroni M, Bruni P, Donati C *et al.* Sphingosine 1-phosphate pathway is dysregulated in adenomyosis. *Reprod Biomed Online* 2022;**45**:15–18.

Xiaoyu L, Weiyuan Z, Ping J, Anxia W, Liane Z. Comparative serum proteomic analysis of adenomyosis using the isobaric tags for relative and absolute quantitation technique. *Fertil Steril* 2013; **100**:505–510.

Yang B, Gu N, Shi S, Zhang C, Chen L, Ouyang J, Lin Y, Sun F, Xu H. Immunoreactivity of plasminogen activator inhibitor 1 and its correlation with dysmenorrhea and lesional fibrosis in adenomyosis. *Reprod Sci* 2021;**28**:2378–2386.

Yoshino O, Yamada-Nomoto K, Kano K, Ono Y, Kobayashi M, Ito M, Yoneda S, Nakashima A, Shima T, Onda T *et al.* Sphingosine 1 phosphate (S1P) increased IL-6 expression and cell growth in endometriotic cells. *Reprod Sci* 2019;**26**:1460–1467.

Zhai J, Vannuccini S, Petraglia F, Giudice LC. Adenomyosis: mechanisms and pathogenesis. *Semin Reprod Med* 2020;**38**:129–143.

Zhang F, Lu Y. The Sphingosine 1-phosphate axis: an emerging therapeutic opportunity for endometriosis. *Reprod Sci* 2023;**30**:2040–2059.

Zhang F, Peng M, Zheng X, Wang X, Liu X, Chen C, Lu Y. Blocking sphingosine 1-phosphate receptor 1 with modulators reduces immune cells infiltration and alleviates endometriosis in mice. *Reprod Biomed Online* 2023;**47**:103304.